

structure of TbTETA assuming fast conformational exchange is at best equal to 47.9% for a rotation angle of the X axis $\alpha = 39^\circ$. The exact nature of the dynamic behavior of PrTETA is unknown at this stage.

Conclusion

The present investigation provides yet another example of the successful application of NMR spectroscopy to structural studies of lanthanide compounds in solution. Despite the low symmetry of the TETA complexes, a quantitative conformational analysis remains feasible provided Yb(III) is the paramagnetic center and provided the complete form of the dipolar equation is used in the calculations.

Only a handful of investigations have permitted complete characterization of the solution behavior of lanthanide complexes. Previous reports deal with the solution structure of lanthanide shift reagents at low temperatures or at room temperature after taking averaging processes into account.⁴ Detailed studies have also been

carried out on organometallic derivatives at -50°C ,¹⁶ on an unusually rigid tris(pyrazolyl) Yb(III) complex,¹⁷ and on the highly symmetric lanthanide tris(pyridine-2,6-dicarboxylates).¹⁸ A variety of complexes can thus be studied by NMR provided the ligands are properly selected to ensure rigidity. In this respect, the polyaza polyacetic macrocycles appear particularly interesting since they form lanthanide complexes that are as rigid as many transition-metal compounds and since they exhibit dynamic behaviors that are readily observed at or above room temperature.

Acknowledgment. J.F.D. is grateful for support by the Fonds National de la Recherche Scientifique of Belgium. J.F.D. is Chercheur Qualifié at this institution.

- (16) Jahn, W.; Yünlü, K.; Oroschin, W.; Amberger, H.-D.; Fischer, R. D. *Inorg. Chim. Acta* **1984**, *95*, 85 and references cited therein.
 (17) Stainer, M. V. R.; Takats, J. *J. Am. Chem. Soc.* **1983**, *105*, 410.
 (18) Desreux, J. F.; Reilley, C. N. *J. Am. Chem. Soc.* **1976**, *98*, 2105.

Contribution from the Department of Chemistry,
 University of Colorado, Boulder, Colorado 80309

Absorption and EPR Spectral Characterization of Tetrasulfur-Bridged Mixed-Valence Dimers of Molybdenum(III/IV). EPR Evidence for Tight Ion Pair Formation in Anionic Systems

Carla J. Casewit and M. Rakowski DuBois*¹

Received April 26, 1985

The electronic properties have been characterized for a series of mixed-valence tetrasulfur-bridged Mo(III)/Mo(IV) dimers of the general formula $[(\text{CpMo})_2(\text{S})_x(\text{SR})_{4-x}]^n$ ($\text{Cp} = \text{C}_5\text{H}_5$, $n = +1, 0, -1$). An absorption in the near-infrared region of the spectrum has been observed for each of the mixed-valence dimers. The relatively narrow peak widths of the absorption bands and the independence of the absorption maxima from solvent dielectric properties have led to the classification of the mixed-valence complexes as completely delocalized (class III) systems. EPR spectra, which show hyperfine coupling to two equivalent molybdenum ions, suggest delocalization on a time scale of 10^7 s^{-1} . The sodium salts of the anionic dimers are proposed to be tight ion pairs in THF on the basis of the observed EPR spectra, which show hyperfine coupling with the counterions. The spectral results are discussed in terms of an extended Hückel molecular orbital description of the dimers.

Introduction

The bridging sulfido ligands of Mo(IV) dimers $[\text{CpMo}(\mu\text{-S})(\mu\text{-SH})_2]$ and $[\text{CpMo}(\mu\text{-S})_2\text{S}_2\text{CH}_2]$ display an extensive reaction chemistry with hydrogen and unsaturated molecules.^{2,3} Although no evidence for coordination of the reactants to the metal ions has been observed, the molybdenum ions are important in regulating the electron density within the Mo_2S_4 core. The addition or dissociation of an unsaturated molecule to or from the sulfur ligands results in a formal two-electron reduction or oxidation, respectively, of the molybdenum centers. The tetrasulfur-bridged molybdenum dimers also display reversible cyclic voltammograms that are characteristic of metal ion oxidation state.⁴ The Mo(IV) dimers undergo one or two reversible one-electron reductions, and the Mo(III) complexes undergo two reversible one-electron oxidations. The ability of the metal ions in these dimeric complexes to reversibly cycle between the +4 and +3 oxidation states is believed to be fundamental to the interaction of sulfido ligands with hydrogen and/or substrate that occurs during the catalysis

of hydrogenation³ and hydrogenolysis^{5,6} reactions by these dimers.

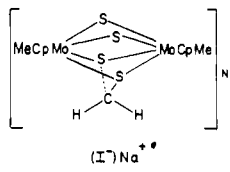
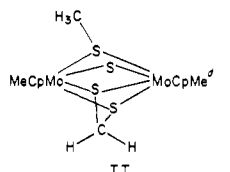
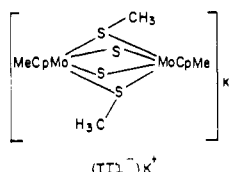
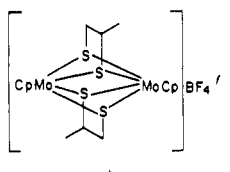
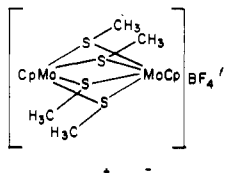
Strong electronic interactions between the molybdenum sites of these complexes may be partly responsible for the observed reaction chemistry and reversible redox processes. Application of the effective atomic number formalism to the tetrasulfur-bridged dimers leads to the postulate of a single bond between Mo(III) ions and a double bond between Mo(IV) ions. The Mo-Mo distances in structurally characterized tetrasulfur-bridged Mo(III), Mo(IV), and mixed valence Mo(III)/Mo(IV) dimers have been found to be essentially invariant to metal ion oxidation state and have values of $\sim 2.60 \text{ \AA}$.^{7,8} Although the distances are compatible with a M-M bonding interaction, the steric constraints of the bridging sulfur ligands preclude using the Mo-Mo distances as reliable indications of direct metal-metal bonding interactions or as indices of bond order.

As part of an effort to understand the general underlying electronic basis for the chemical reactivity and electroactivity of these complexes, and the role of Mo-Mo interactions in particular, we have undertaken a spectroscopic study of the mixed-valence Mo(III)/Mo(IV) dimers shown in Table I. The complexes share

- (1) Alfred E. Sloan Fellow, 1981-1984; Camille and Henry Dreyfus Teacher-Scholar, 1981-1986.
 (2) Rakowski DuBois, M.; VanDerveer, M. C.; DuBois, D. L.; Haltiwanger, R. C.; Miller, W. K. *J. Am. Chem. Soc.* **1980**, *102*, 7456.
 (3) McKenna, M.; Wright, L. L.; Miller, D. J.; Tanner, L.; Haltiwanger, R. C.; Rakowski DuBois, M. *J. Am. Chem. Soc.* **1983**, *105*, 5329.
 (4) Casewit, C. J.; Haltiwanger, R. C.; Noordik, J.; Rakowski DuBois, M. *Organometallics* **1985**, *4*, 119.

- (5) Rakowski DuBois, M. *J. Am. Chem. Soc.* **1983**, *105*, 3710.
 (6) Casewit, C. J.; Coons, D.; Miller, W. K.; Wright, L. L.; Rakowski DuBois, M. *Organometallics*, in press.
 (7) Miller, W. K.; Haltiwanger, R. C.; Vanderveer, M. C.; Rakowski DuBois, M. *Inorg. Chem.* **1983**, *22*, 2973 and references therein.
 (8) Connelly, N. G.; Dahl, L. F. *J. Am. Chem. Soc.* **1970**, *92*, 7470.

Table I. Near-IR Spectra and Electrochemical Properties of Tetrasulfur-Bridged Mixed-Valence Mo(III)/Mo(IV) Dimers

complex	λ_{\max} , nm	ϵ , M ⁻¹ cm ⁻¹	$\Delta\bar{\nu}_{1/2}$, cm ⁻¹ ^a ($\Delta\bar{\nu}_{1/2}$ (calcd), cm ⁻¹) ^b	K_{com} ^c
 (I ⁻)Na ⁺	1360	$\sim 1.0 \times 10^3$	1.4×10^3 (4.1×10^3)	
 II	1360	9.7×10^2	1.8×10^3 (4.1×10^3)	10^{15} ^h
 (III ⁻)K ⁺	1130	1.8×10^3	1.9×10^3 (4.5×10^3)	
 (IV ⁺)BF ₄ ⁻	1040	7.2×10	1.9×10^3 (4.7×10^3)	10^{11} ⁱ
 (V ⁺)BF ₄ ⁻	975	4.0×10	1.8×10^3 ^g (4.9×10^3)	10^{13} ^j

^aThe experimental $\Delta\bar{\nu}_{1/2}$ was determined as described previously: Goldsby, K. A.; Meyer, T. J. *Inorg. Chem.* **1984**, *23*, 3002. ^bEvaluated according to eq 1 in the text. ^c $K_{\text{com}} = \exp(\Delta E_{1/2}/25.69)$ with $\Delta E_{1/2}$ in mV. ^dSolvent THF. ^eThese structural designations are used throughout the paper. ^fThe high-energy side of the band is obscured by a visible band, so $\Delta\nu_{1/2}$ was obtained by doubling the half-bandwidth on the low-energy side. ^g $\Delta E_{1/2}$ taken from ref 4. ^h $\Delta E_{1/2}$ taken from ref 13. The solid-state magnetic moment of $[\text{CpMoSCH}_2\text{CH}(\text{CH}_3)\text{S}]_2^{2+}$ indicates that it has a triplet ground state. The K_{com} thus represents a lower limit. ⁱ $\Delta E_{1/2}$ taken from ref 4 for $[\text{MeCpMo}(\mu\text{-SCH}_3)_2]$.

the same gross structural features; however, the overall charge has been varied, and rather subtle variations in the nature and spatial relationship of the bridging sulfur ligands are present. In this paper, the electronic absorption and EPR spectra and cyclic voltammetric data for the mixed-valence complexes are used to assess the electronic distribution and the extent of metal-metal interaction within the dimers.

Results and Discussion

Near-IR Transitions of Mo(III)/Mo(IV) Dimers. Since the reviews of Robin and Day,⁹ Hush,¹⁰ and Allen and Hush,¹¹ mixed-valence compounds have been the subject of considerable interest.¹² Robin and Day have distinguished three broad classes of mixed-valence complexes⁹ based on the degree of delocalization of the unpaired electron. Several Mo(III)/Mo(IV) tetrasulfur-bridged dimers have been characterized previously,^{4,8,13} but their electronic properties with respect to these classifications have not been investigated in detail. Cyclic voltammetry of the mixed-

valence derivatives shows that reversible electron transfers occur at potentials identical with those of the Mo(III) or Mo(IV) precursors. This suggests that no large structural rearrangements have occurred. Room-temperature solid-state magnetic moment measurements for the air-stable derivatives $[\text{CpMo}(\mu\text{-SCH}_3)_2]_2\text{PF}_6^8$ ((V⁺)PF₆⁻) and $[\text{CpMoSCH}_2\text{CH}(\text{CH}_3)\text{S}]_2\text{BF}_4^{13}$ ((IV⁺)BF₄⁻) indicate that the compounds possess one unpaired electron per dimer as expected for a mixed-valence complex. The crystal structure of each of these derivatives shows crystallographically equivalent molybdenum sites.^{8,13} This observation is consistent with, but not conclusive evidence for, a completely delocalized classification for these dimers, since thermal motions of the atoms may mask slight inequivalencies in distances and angles.

A low-energy absorption band in the near-IR region is observed for each of the mixed-valence molybdenum dimers reported here. Table I lists λ_{\max} values and extinction coefficients for these transitions. Several related equal-valence Mo(III) and Mo(IV) dimers are available for comparison; these do not absorb in the near-IR region of the spectrum. Spectral data for these complexes are discussed below. The energies and intensities of the near-IR transitions are markedly sensitive to ligand type; complexes with the methanedithiolate ligand absorb at the lowest energies, while the perthiolate-bridged derivatives exhibit the highest energy and lowest intensity absorptions.

- (9) Robin, M. B.; Day, P. *Adv. Inorg. Chem. Radiochem.* **1967**, *10*, 247.
 (10) Hush, N. S. *Prog. Inorg. Chem.* **1967**, *8*, 391.
 (11) Allen, G. C.; Hush, N. S. *Prog. Inorg. Chem.* **1967**, *8*, 357.
 (12) For recent reviews see: (a) Creutz, C. *Prog. Inorg. Chem.* **1983**, *30*, 1. (b) Clark, R. J. H. *Chem. Soc. Rev.* **1984**, *13*, 219. (c) Meyer, T. J. *Acc. Chem. Res.* **1978**, *11*, 94.
 (13) Rakowski DuBois, M.; Haltiwanger, R. C.; Miller, D. J.; Glatzmaier, G. *J. Am. Chem. Soc.* **1979**, *101*, 5245.

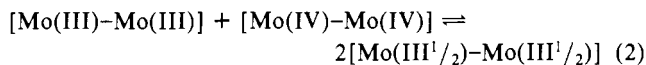
While a low-energy absorption band is a characteristic feature of the electronic spectra of both class II and III mixed-valence complexes, theory indicates that the properties of this band allow one to distinguish between the two classifications. For slightly delocalized class II compounds this absorption corresponds to an intervalence electron transfer, and the energy of the band is related to the rate of thermal electron transfer between the two metal centers. The intervalence-transfer absorptions have properties consistent with the treatment given by Hush.¹⁰ The bands are predicted to be broad with the peak width at half-height equal to or exceeding that given by eq 1. The intervalence-transfer-band

$$\Delta\bar{\nu}_{1/2} = [2310\nu_{\max}]^{1/2} \text{ cm}^{-1} \quad (1)$$

energy is also predicted to vary linearly with changing dielectric properties of the solvent. Completely delocalized class III complexes have equivalent redox sites on the vibrational time scale, and a thermal barrier to intramolecular electron transfer no longer exists. Low-energy absorption bands may appear, but they are described as molecular transitions between delocalized levels. The absorption bands are narrower than predicted by eq 1 and exhibit no solvent dependence.

The measured peak widths at half-height ($\Delta\bar{\nu}_{1/2}$) for the near-IR absorption bands observed for the Mo(III)/Mo(IV) dimers are given in Table I and compared to those predicted by eq 1 for class II systems. The bands are considerably narrower than predicted by the Hush model, supporting a completely delocalized class III formulation. The characteristics of the near-IR bands of the cationic and anionic dimers have been found to be independent of solvent. Although this behavior is also consistent with a class III formulation, relatively little solvent dependency is expected for these transitions on the basis of the theory derived by Hush^{10,12a,14} since the metal-metal distances are relatively short. The neutral complex $(\text{MeCpMo})_2(\mu\text{-SCH}_3)(\mu\text{-S})\text{S}_2\text{CH}_2$ (II) does show a solvent shift: for example, in THF $\nu_{\max} = 7352 \text{ cm}^{-1}$ and in CH_3CN $\nu_{\max} = 7142 \text{ cm}^{-1}$. While the ν_{\max} for class II systems has been both theoretically predicted and experimentally observed to be proportional to the solvent function, the shift observed for $(\text{MeCpMo})_2(\mu\text{-SCH}_3)(\mu\text{-S})\text{S}_2\text{CH}_2$ (II) is inversely related to the solvent dielectric properties.¹⁵

Another diagnostic property of class III mixed-valence systems is a large value of the comproportionation equilibrium (K_{com}) defined in eq 2. Although a number of factors other than



electronic delocalization can determine the value of K_{com} ,¹⁶ special stability of delocalized mixed-valence complexes relative to the fully oxidized and fully reduced forms should result in a large difference between the first and second redox processes relating the equal-valence Mo(III) and Mo(IV) dimers.¹⁶ Quantitative values of K_{com} may be obtained from cyclic voltammetric measurements¹⁷ and are expected to be $>10^3$ for strongly coupled class III systems. For example, the class III oxo-bridged binuclear ruthenium complex $[(\text{NH}_3)_5\text{Ru}-\text{O}-\text{Ru}(\text{NH}_3)_5]^{5+}$ ¹⁸ has $K_{\text{com}} = 10^{34}$. In contrast, $K_{\text{com}} = 100$ for the class II system $\{[\text{Ru}(\text{bpy})_2\text{Cl}]_2\text{pyr}\}^{3+}$.¹⁹ Values of K_{com} for three tetrasulfur-bridged molybdenum dimers have been calculated from cyclic voltammetric data and are presented in Table I. The values, which are $>10^{11}$, are also consistent with a completely delocalized description for the mixed-valence dimers. The previously reported quantitative synthesis of the mixed-valence neutral dimer shown below takes

(14) This fact was noted by a reviewer.

(15) Solvent-dependent shifts of absorption maxima have also been observed for other neutral molybdenum dimers with sulfido ligands (unpublished results). The shifts may be a function of solvent acidity.

(16) Gagne, R. R.; Spiro, C. L.; Smith, T. J.; Hamann, C. A.; Thies, W. R.; Shiemke, A. K. *J. Am. Chem. Soc.* **1981**, *103*, 4073.

(17) Richardson, D. E.; Taube, H. *Inorg. Chem.* **1981**, *20*, 1278.

(18) Baumann, J. A.; Meyer, T. J. *Inorg. Chem.* **1980**, *19*, 345.

(19) Callahan, R. W.; Keene, F. R.; Meyer, J. J.; Salmon, D. J. *J. Am. Chem. Soc.* **1977**, *99*, 1064.

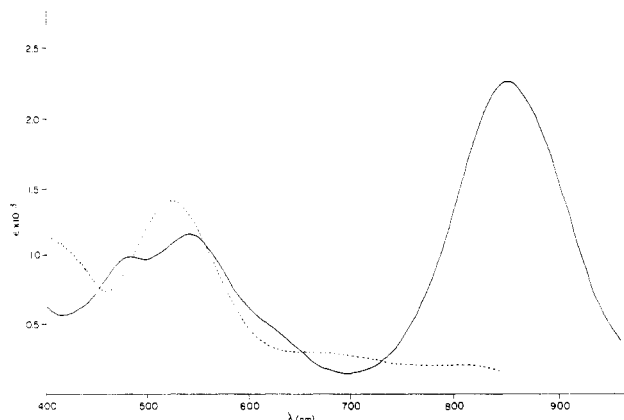


Figure 1. Electronic absorption spectra of the equal-valence Mo(IV) dimer $[(\text{MeCpMo})_2(\mu\text{-S})(\mu\text{-SCH}_3)\text{S}_2\text{CH}_2]\text{I} ((\text{II}^+)\text{I}^-)$ (—) in dichloromethane and the mixed-valence Mo(III)/Mo(IV) dimer $(\text{MeCpMo})_2(\mu\text{-S})(\mu\text{-SCH}_3)\text{S}_2\text{CH}_2$ (II) (---) in THF. The near-IR absorption of II at 1360 nm is not included in this figure.

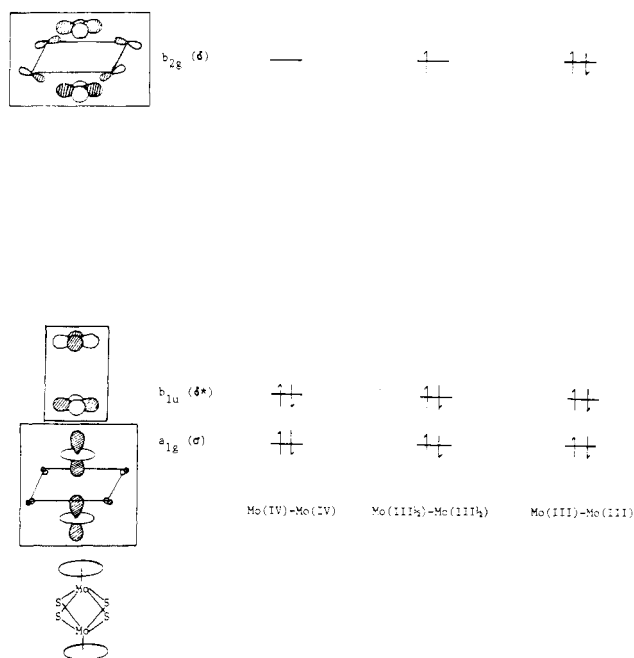
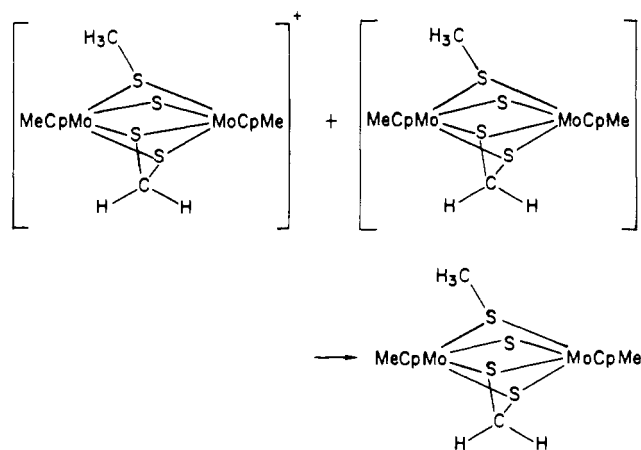


Figure 2. Frontier molecular orbitals and orbital occupancies for tetrasulfur-bridged molybdenum dimers (taken from ref 20).

advantage of the large value of the comproportionation equilibrium for this system:⁴



Visible Spectroscopy. A discussion of the electronic spectral data for the equal-valence molybdenum(IV) and molybdenum(III) dimers serves as a basis for understanding and comparing the

Table II. Electronic Spectral Data for Tetrasulfur-Bridged Molybdenum Dimers

complex	formal metal oxidn state	solvent	λ_{\max} , nm	ϵ , M ⁻¹ cm ⁻¹		
[MeCpMo(μ -S)] ₂ S ₂ CH ₂ (I) ^a	IV	THF	727	2.4 × 10 ³		
			598	2.1 × 10 ³		
			498	8.6 × 10 ²		
[(MeCpMo) ₂ (μ -S)(μ -SCH ₃)S ₂ CH ₂]I ((I ⁺)I ⁻)	IV	CH ₂ Cl ₂	855	2.2 × 10 ³		
			537	1.2 × 10 ³		
			480	9.9 × 10 ²		
[MeCpMo(μ -S)(μ -SCH ₃) ₂] (III)	IV	THF	686	2.8 × 10 ³		
			510	4.4 × 10 ³		
			394	1.3 × 10 ³		
(MeCpMo) ₂ (μ -S)(μ -SCH ₃)S ₂ CH ₂ (II)	III/IV	THF	1360	9.8 × 10 ²		
			523	1.4 × 10 ³		
			~422	~1 × 10 ³ (sh)		
[(MeCpMo(μ -S)) ₂ S ₂ CH ₂]Na ((I ⁻)Na ⁺)	III/IV	THF	1360	~1 × 10 ³ ^b		
			729	~8 × 10 ² ^b		
			400	~2 × 10 ³ (sh)		
[MeCpMo(μ -S)(μ -SCH ₃) ₂]K ((III ⁻)K ⁺)	III/IV	THF	1130	1.8 × 10 ³		
			612	3.0 × 10 ³		
			374	~2 × 10 ³ (sh)		
[CpMoSCH ₂ CH(CH ₃)S] ₂ BF ₄ ((IV ⁺)BF ₄ ⁻)	III/IV	CH ₂ Cl ₂	1040	7.2 × 10		
			618	6.9 × 10 ²		
			480	~3 × 10 ² (sh)		
[CpMo(μ -SCH ₃) ₂]BF ₄ ((V ⁺)BF ₄ ⁻)	III/IV	CH ₂ Cl ₂	408	~5 × 10 ² (sh)		
			975	4.0 × 10		
			543	2.8 × 10 ³		
[(MeCpMo) ₂ (μ -S)(μ -SCH ₃)S ₂ CH ₂]K ((II ⁻)K ⁺)	III	THF	<i>c</i>			
			[CpMoSCH ₂ CH(CH ₃)S] ₂ (IV)	CH ₂ Cl ₂	<i>c</i>	
					[CpMo(μ -SCH ₃) ₂] (V)	CH ₂ Cl ₂

^aStructural designation; structures are shown in Table I. ^bThe measured extinction coefficient represents a lower limit; see Experimental Section. ^cTail of intense UV absorption is observed.

properties of the mixed-valence systems. Table II lists absorbance maxima and extinction coefficients for several tetrasulfur-bridged molybdenum dimers. The visible spectra of the molybdenum(IV) derivatives are characterized by three intense bands in the visible region, while the visible spectra of Mo(III) dimers consist of a relatively featureless UV tail. In the spectra of the analogous mixed-valence Mo(III)/Mo(IV) dimers, two fairly intense absorptions are observed in the visible region in addition to the near-IR band discussed above (Figure 1). As described in the previous section, the properties of the mixed-valence dimers are consistent with completely delocalized ground states, and thus molecular orbital theory provides an appropriate basis for describing their electronic structure. The similarity of the spectra of the mixed-valence and Mo(IV) dimers suggests that both of these complexes might be described by a similar orbital scheme.

Extended Hückel molecular orbital calculations on the model dimers [CpMo^{IV}(μ -S)(μ -SH)]₂ and [CpMo^{III}(μ -SH)]₂ have been reported previously.²⁰ The origin of the lowest energy transitions observed for the Mo(IV) and mixed-valence dimers can be rationalized by examining the frontier molecular orbitals of these models (Figure 2). The frontier molecular orbitals have their major contribution from the metal d orbitals. Mixing of sulfur p-orbital character into the b_{2g} orbital, which involves a δ bond between molybdenum ions, results in a destabilization of this orbital relative to the b_{1u} orbital, which involves a δ^* interaction between metal ions. The latter orbital is the HOMO in the molybdenum(IV) dimers. The relatively intense, lowest energy band observed for these dimers in the visible region and for the mixed-valence Mo(III)/Mo(IV) complexes in the near-IR region is assigned to the $\delta^* \rightarrow \delta$ transition, which is electric dipole allowed in idealized D_{4h} symmetry. Because of the nature of the molecular orbitals involved, this transition also has some metal to ligand charge-transfer character. The b_{2g} orbital is fully occupied in the Mo(III) dimers, and no low-energy transitions are observed for these systems.

The trend toward lower intensity absorption bands noted above for the mixed-valence perthiolate-bridged derivatives is consistent

Table III. Reduction Potentials (E_R) and Lowest Optical Transition Energies (E_{hv}) of the Tetrasulfur-Bridged Molybdenum(IV) Dimers

complex	E _R ^a	E _{hv} ^b
[(MeCpMo) ₂ (μ -S)(μ -SCH ₃)S ₂ CH ₂]I ((II ⁺)I ⁻)	-0.34	1.45
(MeCpMo(μ -S)) ₂ S ₂ CH ₂ (I)	-1.30	1.71
[MeCpMo(μ -S)(μ -SCH ₃) ₂] (III)	-1.43	1.81

^aIn V vs. SCE; data taken from ref 4. ^bIn eV; data taken from this work.

with the calculated observation that the contribution to the b_{2g} orbital from the sulfur ligands—and therefore, the charge-transfer character of the transition—decreases as sulfido ligands are substituted by thiolates. An inversion in the ordering of the nearly degenerate σ and δ^* levels for these complexes is also a possibility. This would also result in a decrease in intensity due to the forbidden nature of the a_{1g} → b_{2g} transition.

The molecular orbital scheme presented above suggests that variation of the sulfur ligands within a series of molybdenum(IV) dimers will change the energy of the LUMO while the HOMO remains relatively unaffected. It would therefore be of interest to consider whether the energies of the absorption maxima show a correlation with the electrochemical potentials for a series of Mo(IV) dimers. It has been pointed out previously that comparisons of optical transition energies and electrochemical potentials do not always show a meaningful correlation, even for a series of closely related compounds; the latter thermodynamic data may not be related to simple orbital energy differences if factors such as solvation energies, entropy changes, and electron repulsion terms do not remain constant within the series.²¹ Assumptions implied in such comparisons have been discussed in more detail elsewhere.²² Nevertheless, other complexes with a similar situation for frontier molecular orbitals, that is, for which the LUMO varies with ligand substituents while the HOMO is relatively unaffected, have shown useful correlations between electrochemical and electronic absorption data.²¹

(20) DuBois, D. L.; Miller, W. K.; Rakowski DuBois, M. *J. Am. Chem. Soc.* **1981**, *103*, 3429.

(21) Templeton, J. L.; Herrick, R. S.; Morrow, J. R. *Organometallics* **1984**, *3*, 535.
(22) (a) Vlček, A. A. *Electrochim. Acta* **1968**, *13*, 1063. (b) Masek, J. *Inorg. Chim. Acta, Rev.* **1969**, *3*, 99.

Table IV. EPR Spectral Data for Mo(III)/Mo(IV) Dimers

complex	solvent ^a	temp, °C	<i>g</i> ^b	<i>A</i> _{Mo} , G	<i>A</i> _{alkali M} , G
[CpMo(μ-SCH ₃) ₂] ₂ BF ₄ ((V ⁺)BF ₄) ^c	CH ₂ Cl ₂	-60	2.007	18	
[MeCpMo(μ-S)(μ-SCH ₃) ₂] ₂ Na ((III ⁻)Na ⁺)	THF	room	2.004	15	4
(MeCpMo) ₂ (μ-S)(μ-SCH ₃) ₂ S ₂ CH ₂ (II)	THF	-60	1.993	14	
[(MeCpMo(μ-S)) ₂ S ₂ CH ₂] ₂ Na ((I ⁻)Na ⁺)	THF	room	1.986	15	15
[(MeCpMo(μ-S)) ₂ S ₂ CH ₂] ₂ K ((I ⁻)K ⁺)	THF	room	1.984	15	4

^a Concentration range 10⁻²-10⁻⁴ M. ^b Referenced to external solid DPPH. ^c Structural designation (structures shown in Table I).

Unfortunately, only three molybdenum(IV) dimers with reversible reduction potentials and singlet ground states are available for comparison in this context. It is interesting that a plot of their Mo(IV)/Mo(IV)-Mo(IV)/Mo(III) reduction potentials vs. the lowest optical transition energies shows a good correlation (correlation coefficient 0.99, Table III). The observed value of the slope of the above plot is 3, while a value of 1 is predicted for a situation in which the energy of the HOMO remains constant. Our results from this very limited data set suggest that the structural and electronic variations introduced by the change in sulfur ligands also perturb to a lesser extent the energy of the HOMO in this series of dimers. Further synthetic work may eventually lead to a more extensive data set, which will be necessary for a better understanding of the influence of ligand and charge on these spectral and electrochemical parameters.

For the two molybdenum(IV) dimers for which both reversible oxidation and reduction processes are observed, (CpMo(μ-S))₂S₂CH₂ (I) and (CpMo(μ-S))₂(μ-SCH₃)₂ (III), the differences in measured oxidation and reduction potentials⁴ lead to an estimate of the HOMO-LUMO gaps of 12 660 and 16 130 cm⁻¹ (790 and 620 nm), respectively. In these cases the calculated values compare reasonably well with the observed transitions at 727 and 685 nm, respectively.

EPR Spectra of Mo(III)/Mo(IV) Dimers. The EPR parameters obtained for solutions of the tetrasulfur-bridged Mo(III)/Mo(IV) dimers are collected in Table IV. All of the spectra show features due to coupling of the unpaired electron with two equivalent molybdenum nuclei. The spectra consist of an intense central signal due to the statistically predominant dimer in which *I*_{Mo1} = *I*_{Mo2} = 0. Hyperfine coupling in the less abundant dimer with *I*_{Mo1} = 0, *I*_{Mo2} = 5/2 (and vice versa) leads to a lower intensity sextet. The integrated intensity of these hyperfine lines is diagnostic. The intensities of the sextet relative to the central signal for an electron delocalized over two molybdenums is expected and observed to be twice as high as for an electron localized on one metal atom.²³ Additional evidence for the electron being delocalized over two molybdenum nuclei comes from the observation of a very low intensity 11-line spectrum due to coupling of the unpaired electron with two equivalent *I*_{Mo1} = 5/2, *I*_{Mo2} = 5/2 nuclei (e.g., Figure 3).

A featureless EPR spectrum of [CpMo(μ-SCH₃)₂]₂⁺ (V⁺) has previously been reported by Connelly and Dahl⁸ and Dessy et al.²⁴ Our measured *g* value of 2.007 for a 1.8 × 10⁻⁴ M solution of the BF₄ salt in dichloromethane is in close agreement with those found by the previous workers. In addition, we were able to observe hyperfine structure similar to that reported for the other mixed-valence dimers (see Table IV) by cooling the solution to -60 °C. In contrast, we were unable to obtain an EPR spectrum for the complex [CpMoSCH₂CH(CH₃)S]₂BF₄ ((IV⁺)BF₄⁻), even at -60 °C in dichloromethane over a concentration range of 4 × 10⁻³-4 × 10⁻⁵ M.²⁵ Other characterization data suggest the complex is structurally and electronically similar to [CpMo(μ-SCH₃)₂]₂BF₄ ((V⁺)BF₄⁻). Room-temperature magnetic susceptibility mea-

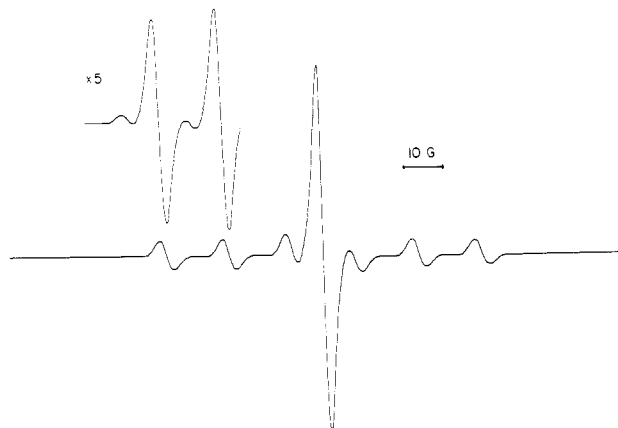


Figure 3. X-Band EPR spectrum of [MeCpMo(μ-S)(μ-SCH₃)₂]₂K ((III⁻)K⁺) in THF at 25 °C. Inset shows 2 of 11 very weak hyperfine lines resulting from electron coupling to both molybdenum nuclei with *I* = 5/2.

surements in solution and in the solid state confirm the presence of a single unpaired electron. Plots of absorbance vs. concentration for the visible data indicate that the complex obeys Beer's law in acetonitrile solution. X-ray crystallography and cyclic voltammetry support the structural integrity of the dimer in the solid state and in solution.¹³ Our inability to observe an EPR signal for this complex may be due to a spin-exchange broadening process or to unfavorable spin-lattice relaxation times.²⁶ Further information on the system may require very low temperature EPR and magnetic susceptibility studies.

The magnitudes of the molybdenum hyperfine coupling constants observed in the EPR spectra of the molybdenum dimers (*A* = 14-18 G) are suggestive of some ligand contribution to the spin density. For example, the *A* values are smaller than those observed for the delocalized Mo(III)/Mo(IV) dimer [Mo₂(μ-SO₂)(μ-S₂)(CN)₈]⁻ (*A* = 22 G)²⁷ and for delocalized Mo(III)/Mo(II) dimers^{23,28} (e.g., for [Mo₂(SO₄)₄]³⁻, *A*_{||} = 48 G and *A*_⊥ = 24 G). The values are also less than half the magnitude observed for most monomeric Mo(V) complexes.²⁹ The variation in *A* is small for these tetrasulfur-bridged dimers, and there are no obvious trends in the magnitude. These observations suggest that the spin densities on molybdenum do not vary significantly with ligand structure, despite some delocalization onto the ligands.

We were interested in determining the amount of unpaired spin density located on the sulfur ligands in the dimers. Because the natural abundance of the spin-active sulfur isotope is very low (³³S, *I* = 3/2, natural abundance 0.74%), EPR spectra of the unlabeled complexes are not expected to show coupling to the sulfur ligands.³⁰ However, we have found that the anionic

- (23) Cotton, F. A.; Frenz, B. A.; Pedersen, E.; Webb, T. R. *Inorg. Chem.* **1975**, *14*, 391.
 (24) Dessy, R. E.; Kornmann, R.; Smith, C.; Haytor, R. *J. Am. Chem. Soc.* **1968**, *90*, 2001.
 (25) A very weak EPR signal is observed for old samples of [CpMoSCH₂CH(CH₃)S]₂BF₄ in CH₂Cl₂ solution: *g* = 1.986, *A*_{Mo} = 37 G. The intensities of the hyperfine lines are characteristic of an electron interacting with one molybdenum nucleus. This EPR-active species has not been identified.

- (26) Drago, R. S. "Physical Methods in Chemistry"; W. B. Saunders: Philadelphia, 1977; p 316.
 (27) Müller, A.; Eltzner, W.; Jostes, R.; Bogge, H.; Dieman, E.; Schimanski, J.; Leuken, H. *Angew. Chem., Int. Ed. Engl.* **1984**, *23*, 389.
 (28) Cotton, F. A.; Pedersen, E. *Inorg. Chem.* **1975**, *14*, 399.
 (29) (a) Stiefel, E. I. *Prog. Inorg. Chem.* **1977**, *22*, 1. (b) Spence, J. T.; Minelli, M.; Rice, C. A.; Chasteen, N. C.; Scullane, M. In "Molybdenum Chemistry of Biological Significance"; Newton, W. E., Otsuka, S., Eds.; Plenum Press: New York, 1980; p 263.
 (30) Natural-abundance ³³S hyperfine splitting has been observed in single-crystal EPR studies of Cu(II) complexes having CuS₄ coordination: Stach, J.; Kirmse, R.; Dietzsch, W.; Olk, R.; Hoyer, E. *Inorg. Chem.* **1984**, *23*, 4779 and references within.

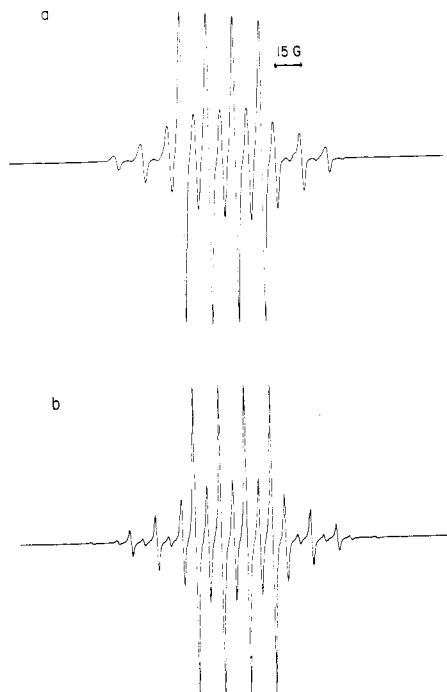


Figure 4. (a) X-Band EPR spectrum of $[(\text{MeCpMo}(\mu\text{-S}))_2\text{S}_2\text{CH}_2]\text{Na}$ ($(\text{I}^-)\text{Na}^+$) in THF at 25 °C. (b) Simulated spectrum.

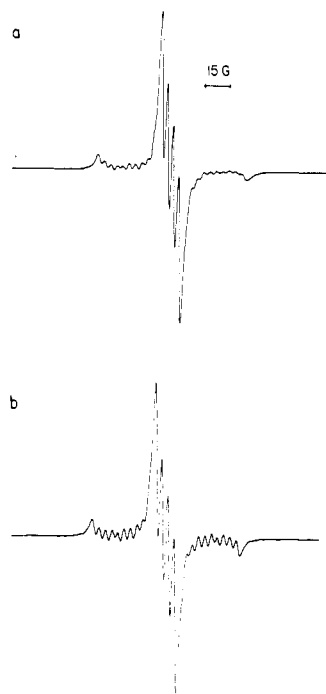


Figure 5. (a) X-Band EPR spectrum of $[(\text{MeCpMo}(\mu\text{-S}))_2\text{S}_2\text{CH}_2]\text{K}$ ($(\text{I}^-)\text{K}^+$) in THF at 25 °C. (b) Simulated spectrum.

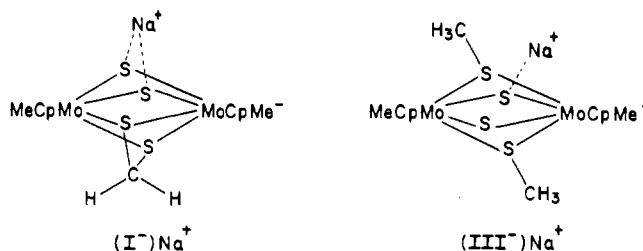
mixed-valence dimers have spectral features that provide indirect evidence for spin density on the sulfido ligands.

The EPR spectra of $[(\text{MeCpMo}(\mu\text{-S}))_2\text{S}_2\text{CH}_2]^-$ (I^-) in THF are more complex than expected for an electron interacting with two equivalent molybdenum nuclei. Experimental and simulated spectra of the sodium salt are reproduced in Figure 4. In addition to the molybdenum hyperfine coupling of 15 G, the spectrum shows hyperfine features from coupling to the associated sodium counterion with spin $3/2$ ($A_{\text{Na}} = 15$ G). The spectrum demonstrates that this complex should be formulated as a tight ion pair in THF. A weaker hyperfine coupling to the counterion is also observed in the spectrum of the analogous potassium salt in THF solution (Figure 5). Spectral simulation gives $A_{\text{Mo}} = 15$ G and $A_{\text{Na}} = 4$ G. If only a Fermi contact contribution to the coupling

is assumed, the ratio of spin densities at the counterion and molybdenum nuclei can be calculated. For both the sodium and potassium salts discussed here, the spin density at the counterion nucleus is found to be $\sim 1/4$ that at the molybdenum nuclei. A counterion dependence of the maximum of the near-IR absorption for $[(\text{MeCpMo}(\mu\text{-S}))_2\text{S}_2\text{CH}_2]^-$ (I^-) in THF is also observed. The maxima for the sodium and potassium salts are 1360 and 1295 nm, respectively.

The constituent ions of $[(\text{MeCpMo}(\mu\text{-S}))_2\text{S}_2\text{CH}_2]\text{K}$ ($(\text{I}^-)\text{K}^+$) are solvent-separated in the higher dielectric medium acetonitrile. The room-temperature EPR spectrum of the salt generated in situ in this solvent (concentration $\sim 10^{-3}$ M) shows no hyperfine coupling to potassium ion. Instead a spectrum characteristic of an electron delocalized over two equivalent molybdenum nuclei is observed with an A_{Mo} value identical with that measured for the THF solution.

The closely related mixed-valence salt $[(\text{MeCpMo}(\mu\text{-S}))_2(\mu\text{-SCH}_3)_2]\text{Na}$ ($(\text{III})\text{Na}^+$) also shows hyperfine coupling to the sodium counterion, but the coupling constant of 4 G is much smaller than that observed for the sodium salt of $[(\text{MeCpMo}(\mu\text{-S}))_2\text{S}_2\text{CH}_2]^-$ (I^-). Stronger ion pair formation may be possible for the latter complex through interaction with two adjacent sulfido ligands, as shown in structure I. Since the methanethiolate ligands



are in trans positions in $[(\text{MeCpMo}(\mu\text{-S})(\mu\text{-SCH}_3)_2)]_2^-$ (structure III), a chelating interaction of sulfido ligands with the counterion is not possible.²

Identification of anionic transition-metal complex ion pairs has been accomplished by IR analysis of carbonyl complexes and clusters.^{31,32} However, very few paramagnetic transition-metal ion pairs have been identified by EPR spectroscopy. For example, IR analysis of the mixed-valence dimer $[\text{CpCo}(\text{CO})]_2\text{Na}$ shows that it is a tight ion pair in THF.³² The EPR spectrum of this complex in the same solvent shows no coupling to the sodium counterion, presumably because no spin density resides on the carbonyl ligands. In contrast, the EPR spectrum of $\text{Cp}_2\text{TiH}_2\text{Na}$ shows hyperfine coupling to both the hydride ligands and to the sodium counterion ($A_{\text{Na}} = 6.7$ G).³³ This system provides the only previous example that we have found of EPR verified ion pairing in an organometallic salt. The existence of a large number of aromatic hydrocarbon ion pairs in solvents of low dielectric constant has been demonstrated by EPR.³⁴ The Na and K hyperfines that have been observed for these organic ion pairs are, in general, quite small (< 2 G). The larger hyperfines observed for $[(\text{MeCpMo}(\mu\text{-S}))_2\text{S}_2\text{CH}_2]^-$ (I^-) and $\text{Cp}_2\text{TiH}_2\text{Na}$ may be a consequence of the chelation of the alkali metal by the sulfido and hydrido ligands, respectively.

Summary. The tetrasulfur-bridged molybdenum dimers provide an unusual opportunity to consider electronic absorption data for an extensive series of equal-valence and mixed-valence dimers in terms of a molecular orbital description. The description of the frontier molecular orbitals derived from extended Hückel calculations has provided a very useful framework for understanding

- (31) (a) Darensbourg, M. Y.; Darensbourg, D. J.; Burns, D.; Drew, D. A. *J. Am. Chem. Soc.* **1976**, *98*, 3127. (b) Kao, S. C.; Darensbourg, M. Y.; Schenk, W. *Organometallics* **1984**, *3*, 871. (c) Schick, K.-P.; Jones, N. L.; Sekula, P.; Boag, N. M.; Labinger, J. A.; Kaesz, H. D. *Inorg. Chem.* **1984**, *23*, 2204.
- (32) Schore, N. E.; Ilenda, C. S.; Bergman, R. G. *J. Am. Chem. Soc.* **1977**, *99*, 1781.
- (33) Kenworthy, J. G.; Myatt, J.; Symons, M. C. R. *J. Chem. Soc. A* **1971**, 1020.
- (34) (a) Symons, M. C. R. *J. Phys. Chem.* **1967**, *71*, 172. (b) DeBoer, E. *Adv. Organomet. Chem.* **1964**, *2*, 115.

the unusual reactivity of the dimers.²⁰ In particular, the nature of the contribution of the sulfur p orbitals to the LUMO of the Mo(IV) complexes is consistent with the extensive reactivity of the sulfido ligands in these dimers with hydrogen and with unsaturated molecules. The studies reported here confirm the validity of the molecular orbital description of these systems. The electronic and EPR spectra and the cyclic voltammetric data for the Mo(III)/Mo(IV) tetrasulfur-bridged derivatives provide evidence for delocalization of the unpaired electron over two equivalent molybdenum ions. The EPR results for the anionic Mo(III)/Mo(IV) complexes, which show hyperfine coupling to the counterions presumably as a result of the ions' interaction with sulfido ligands, provide the first spectral corroboration for the proposed description of the reactive b_{2g} frontier molecular orbital in these dimers.

Experimental Section

Materials. Tetrahydrofuran was distilled from calcium hydride prior to use. Dichloromethane was distilled over P_2O_5 or passed through an activated alumina column. Acetonitrile was dried over calcium hydride, filtered, and distilled from P_2O_5 . Spectral grade acetone and methanol were used without further purification. Potassium graphite was obtained from Alfa, and dry NaH was purchased from Aldrich.

Physical Measurements. EPR spectra were recorded on a Varian E-109 X-band spectrometer. The g values were measured relative to solid DPPH ($g = 2.0036$). Air-sensitive solutions of $(MeCpMo)_2(\mu-S)(\mu-SCH_3)S_2CH_2$, $[(MeCpMo)(\mu-SCH_3)(\mu-S)]_2^-$, and $[MeCpMo(\mu-S)]_2S_2CH_2^-$ were transferred to an EPR tube fitted with a ground-glass stopper under a nitrogen atmosphere in a Vacuum Atmospheres glovebox. EPR spectra were recorded immediately. The simulated EPR spectra were generated with use of a first-order spin Hamiltonian. The absorption spectra due to the various isotopic and spin possibilities were superimposed with the appropriate population factors. A Lorentzian line shape function (line width 1 G for $(I^-)Na^+$, line width 2.6 G for $(I^-)K^+$) was used. Finally the absorption spectra were numerically differentiated to obtain the spectra plotted in Figures 4 and 5.

Electronic spectra were obtained in matched cells with Cary 14 and Cary 219 spectrophotometers. Air-sensitive solutions were transferred to a cell fitted with a Kontes high-vacuum valve under a nitrogen at-

mosphere in a Vacuum Atmospheres glovebox. Spectra were recorded immediately.

Syntheses. The syntheses of the Mo(IV),²⁻⁴ Mo(III),^{4,8,13} and cationic^{8,13} and neutral⁴ mixed-valence dimers were carried out according to literature methods. The anionic mixed-valence dimers were generated in solution as described below.

$[MeCpMo(\mu-S)(\mu-SCH_3)]_2K^-(III^-)K^+$. THF and CH_3CN Solutions of the title complex were generated in a glovebox by reduction of solutions of $[MeCpMo(\mu-S)(\mu-SCH_3)]_2$ (III) with excess KC_8 . The reduced teal blue solutions were filtered through a glass wool plug before spectral analysis. Comparison of the visible absorption spectra for the neutral and anionic derivatives served as a check on the completeness of reduction. The purity of the anion was inferred from its spectroscopically observed quantitative oxidation to the neutral starting material upon exposure to air.

$[MeCpMo(\mu-S)]_2S_2CH_2^-(I^-)$. THF and CH_3CN solutions of the title anion were generated in a glovebox by reduction of solutions of $[MeCpMo(\mu-S)]_2S_2CH_2$ (I) with excess KC_8 or NaH. The green solutions were filtered through a glass wool plug before spectral analysis. Exposure of THF solutions of the anion to air resulted in oxidation to neutral starting material. However, under these conditions the starting material undergoes partial further oxidation to an unidentified yellow complex. Since the starting material was not regenerated quantitatively, it was difficult to determine whether or not a small amount of air oxidation of the anion had taken place before electronic spectra were recorded. The reported extinction coefficients are lower limits, with estimated errors of <20%.

Acknowledgment. This work has been supported by the National Institutes of Health, by the National Science Foundation, and in part by the donors of the Petroleum Research Fund, administered by the American Chemical Society. M.R.D. is grateful for a fellowship from the John Simon Guggenheim Foundation, 1984-1985. We are grateful to A. K. Rappé for providing us with the EPR simulation program.

Registry No. I, 85565-70-4; $(I^-)Na^+$, 99510-47-1; $(I^-)K^+$, 99495-31-5; II, 99510-48-2; $(II^-)I^-$, 99510-49-3; $(II^-)K^+$, 99495-28-0; III, 99495-27-9; $(III^-)K^+$, 99495-22-4; IV, 99495-29-1; $(IV^+)BF_4^-$, 99495-24-6; V, 99495-30-4; $(V^+)BF_4^-$, 99495-26-8.

Contribution from the Department of Chemistry,
University of Wisconsin—Madison, Madison, Wisconsin 53706

Host-to-Guest, Excited-State Energy Transfer in Lamellar Solids. Photoluminescent Properties of Hydrated Europium Uranyl Phosphate

Michael M. Olken, Carla M. Verschoor, and Arthur B. Ellis*

Received July 23, 1985

Hydrogen uranyl phosphate (HUP) undergoes complete exchange with Eu^{3+} ions to yield a hydrated, lamellar solid of approximate composition $Eu_{1/3}UO_2PO_4$ (EuUP). An X-ray powder pattern of the solid indicates the presence of a single phase, which indexes in tetragonal symmetry with an interlamellar spacing of ~ 10.2 Å. Exclusive excitation of the host UO_2^{2+} chromophore leads to photoluminescence (PL) from both excited UO_2^{2+} and Eu^{3+} , indicative of host-to-guest, excited-state energy transfer. From radiative quantum yields and time-resolved PL measurements, energy transfer is estimated to occur with nearly unit efficiency at a rate of $\sim 2 \times 10^5$ s⁻¹. High-resolution PL data obtained at 12 K indicate that the Eu^{3+} ions can occupy multiple lattice sites in EuUP.

Introduction

The rich diversity of intercalation chemistry¹ has prompted us to explore the excited-state properties of lamellar solids. We recently reported on the photoluminescence (PL) of the layered compound hydrogen uranyl phosphate (HUP), $HUO_2PO_4 \cdot 4H_2O$, and of solids derived therefrom by cationic substitution.²⁻⁴ A partially substituted solid, $H_{0.7}[Cr(NH_3)_6]_{0.1}UO_2PO_4 \cdot 6H_2O$ (HCrUP), provided evidence for efficient host-to-guest energy transfer: excitation of the host UO_2^{2+} chromophore yielded PL and an aquation reaction characteristic of the guest Cr(III) complex.^{3,4}

Our results with HCrUP prompted us to examine whether other classes of trivalent cations capable of involvement in energy-transfer processes could be incorporated into lamellar solids derived from HUP. Lanthanion ions are attractive candidates in this regard. Our initial choice for such studies was Eu(III), since energy transfer from UO_2^{2+} to Eu^{3+} ions is well documented in a variety of media including solutions,⁵ solids having the perovskite

- (1) For an overview, see: "Intercalation Chemistry"; Whittingham, M. S., Jacobson, A. J., Eds.; Academic Press: New York, 1982.
- (2) Olken, M. M.; Biagioni, R. N.; Ellis, A. B. *Inorg. Chem.* **1983**, *22*, 4128.
- (3) Olken, M. M.; Ellis, A. B. *J. Am. Chem. Soc.* **1984**, *106*, 7468.
- (4) Olken, M. M.; Verschoor, C. M.; Ellis, A. B. *J. Lumin.* **1984**, *31/32*, 552.

* To whom correspondence should be addressed.